

# Three-component fractional quantum Hall effect in topological flat bands

Tian-Sheng Zeng<sup>1</sup>

<sup>1</sup>*Department of Physics, College of Physical Science and Technology, Xiamen University, Xiamen 361005, China*  
(Dated: July 12, 2024)

We study the many-body ground states of three-component quantum particles in two prototypical topological lattice models under strong intercomponent and intracomponent repulsions. At band filling  $\nu = 3/4$  for hardcore bosons, we demonstrate the emergence of three-component fractional quantum Hall (FQH) effect characterized by the  $\mathbf{K}$  matrix, through exact diagonalization study of four-fold quasidegenerate ground states with a robust spectrum gap and the combined density-matrix renormalization group calculation of fractional drag charge pumping. Further we formulate the topological characterization of FQH states of three-component Bose-Fermi mixtures at various fillings by the  $\mathbf{K}$  matrix. At last we discuss the possible generalization of our approach to identify non-Abelian three-component spin-singlet FQH states.

## I. INTRODUCTION

Since Halperin's classic proposal of two-component quantum Hall effect [1], the occurrence of multicomponent fractional quantum Hall (FQH) effects gradually comes into the eyesight of humankind when an internal degree of freedom (i.e. spin and layer) is included [2–8]. Subsequently, after the experimental discovery of a rich class of approximately SU(4) symmetric FQH effects in graphene sheets with two-fold spin and two-fold valley degrees of freedom [9, 10], many theoretical investigations proposed a generalization of Halperin's wave functions to four-component component cases, such as SU(4) composite-fermion construction [11] and SU(4) generalization of Halperin's trial wavefunction [12, 13]. Nevertheless multicomponent quantum Hall systems offer us a new scope for seeking topological phases that have no analogue in one-component systems. [14]. Indeed, several exotic interlayer-correlated FQH effects have been experimentally observed in two separated parallel graphene layers [15, 16]. Among these multicomponent FQH systems, different intercomponent and intracomponent correlations play the vital role. However most of the prior active studies focus on exploring even-component cases including two-component bosonic quantum Hall effect like Halperin (221) FQH effect [17–20], bosonic integer quantum Hall effect [19–23] and even non-Abelian spin-singlet quantum Hall effects (dubbed as NASS states) [24–26]. To date, much little knowledge about three-component FQH effects are acquired, due to relatively rare clear-cut examples [27].

In a parallel route, the exciting arise of topological Chern bands (such as realization of Haldane Chern insulator [28] and observation of fractional quantum anomalous Hall effect with an internal spin-valley locking degree of freedom in moiré superlattices [29, 30]) in analogy to two-dimensional Landau levels endows us prime candidate for studying multicomponent quantum Hall effects. In particular, it is numerically suggested that FQH effects at specific band fillings  $\nu = 1/(C + 1)$  (for spinless hardcore bosons) and  $\nu = 1/(2C + 1)$  (for spinless fermions) in topological flat bands with high Chern num-

bers  $C > 1$ , are described as color-entangled lattice versions of  $C$ -component FQH effects where  $C$  serves as an internal degree of freedom [31–38]. However, a closely related drawback is that it is hard to directly discern mutual particle correlations contributing from each component in these lattice models. Alternatively, we may consider multicomponent quantum particles loaded in topological flatbands with Chern number  $C = 1$  as the substitute. The merit of these models is that now we can distinguish intercomponent and intracomponent correlations in a designed many-body Hamiltonian. Extensive numerical calculations have demonstrated FQH effects of multicomponent quantum particles in topological flat bands with unit Chern number [39–44], which are characterized by the  $\mathbf{K}$ -matrix within the framework of the Chern-Simons gauge-field theory [45–49]. Moreover, the  $\mathbf{K}$ -matrix also solely determines the modular matrix which encodes the statistics of anyonic excitations for multicomponent FQH states [50]. Interestingly, recent studies also suggest that two-component Bose-Fermi mixtures in topological bands can host exotic chiral topological phases [51, 52]. A spectacular question is that whether there exist new kinds of fascinating FQH effects in three-component systems or not.

Here, we aim at searching for different possible exotic three-component FQH effects at various filling factors in topological lattice models with the lowest band carrying unit Chern number  $C = 1$ , and then further identify their topological properties. This paper is organized as follows. In Sec. II, we introduce the microscopic interacting Hamiltonian of three-component quantum particles loaded on two prototypical topological lattice models, and give a description of our numerical methods. In Sec. III, we discuss the FQH states of three-component bosons, and present numerical results of their topological characterization based on the  $\mathbf{K}$  matrix by exact diagonalization and density-matrix renormalization group calculations. In Sec. IV, we discuss the identification of more exotic FQH effects of three-component Bose-Fermi mixtures based on the  $\mathbf{K}$  matrix; following that, we present our numerical results for a mixture of two-component bosons and one-component fermions in Sec. IV A, and

a mixture of one-component bosons and two-component fermions in Sec. IV B. In Sec. V, we discuss the non-Abelian spin-singlet FQH effect. Finally, we present a summary and discussion in Sec. VI, and discuss the possible multicomponent quantum Hall effect.

## II. MODEL AND METHOD

In this section, we begin with the description of three-component quantum particles (either bosons or fermions) with strong intercomponent and intracomponent repulsions in topological flat bands, and introduce our density-matrix renormalization group (DMRG) and exact diagonalization (ED) simulations. We study two different prototypical topological lattice models, i.e.  $\pi$ -flux checkerboard (CB) lattice [53] and Haldane-honeycomb lattice [54]. The model Hamiltonian is formulated as

$$H_{CB} = \sum_{\sigma} \left[ -t \sum_{\langle \mathbf{r}, \mathbf{r}' \rangle} e^{i\phi_{\mathbf{r}'\mathbf{r}}} c_{\mathbf{r}',\sigma}^{\dagger} c_{\mathbf{r},\sigma} - \sum_{\langle\langle \mathbf{r}, \mathbf{r}' \rangle\rangle} t'_{\mathbf{r},\mathbf{r}'} c_{\mathbf{r}',\sigma}^{\dagger} c_{\mathbf{r},\sigma} - t'' \sum_{\langle\langle\langle \mathbf{r}, \mathbf{r}' \rangle\rangle\rangle} c_{\mathbf{r}',\sigma}^{\dagger} c_{\mathbf{r},\sigma} + H.c. \right] + V_{int}, \quad (1)$$

$$H_{HC} = \sum_{\sigma} \left[ -t \sum_{\langle \mathbf{r}, \mathbf{r}' \rangle} c_{\mathbf{r}',\sigma}^{\dagger} c_{\mathbf{r},\sigma} - t' \sum_{\langle\langle \mathbf{r}, \mathbf{r}' \rangle\rangle} e^{i\phi_{\mathbf{r}'\mathbf{r}}} c_{\mathbf{r}',\sigma}^{\dagger} c_{\mathbf{r},\sigma} - t'' \sum_{\langle\langle\langle \mathbf{r}, \mathbf{r}' \rangle\rangle\rangle} c_{\mathbf{r}',\sigma}^{\dagger} c_{\mathbf{r},\sigma} + H.c. \right] + V_{int}, \quad (2)$$

with the many-body interaction given by

$$V_{int} = U \sum_{\sigma \neq \sigma'} \sum_{\mathbf{r}} n_{\mathbf{r},\sigma} n_{\mathbf{r},\sigma'} + \sum_{\sigma} V_{\sigma} \sum_{\langle \mathbf{r}, \mathbf{r}' \rangle} n_{\mathbf{r}',\sigma} n_{\mathbf{r},\sigma}, \quad (3)$$

Here  $\langle \dots \rangle$ ,  $\langle\langle \dots \rangle\rangle$  and  $\langle\langle\langle \dots \rangle\rangle\rangle$  denote the nearest-neighbor, next-nearest-neighbor, and next-next-nearest-neighbor pairs of sites, and we choose the corresponding tunnel couplings  $t' = 0.3t$ ,  $t'' = -0.2t$ ,  $\phi = \pi/4$  for checkerboard lattice and  $t' = 0.6t$ ,  $t'' = -0.58t$ ,  $\phi = 2\pi/5$  for honeycomb lattice respectively [54], whose lowest band is rather flat and host a Chern number  $C = 1$ . The subscript labels  $\sigma = 0, \pm 1$  are used as the pseudospin indices to distinguish different components,  $c_{\mathbf{r},\sigma}^{\dagger}$  is the particle creation operator of the spin- $\sigma$  component at site  $\mathbf{r}$ ,  $n_{\mathbf{r},\sigma} = c_{\mathbf{r},\sigma}^{\dagger} c_{\mathbf{r},\sigma}$  is the particle number operator of the spin- $\sigma$  component at site  $\mathbf{r}$ .  $U$  is the strength of the onsite intercomponent repulsion, and  $V_{\sigma}$  is the intracomponent repulsion strength between the nearest-neighbor pairs of the spin- $\sigma$  component.

In our numerical calculations, we fix the global particle number  $N_{\sigma}$  for each component (that means our models are constrained by  $U(1) \times U(1) \times U(1)$  symmetry), and take the finite lattice systems with  $N_x \times N_y$  unit cells (then  $N_s = 2 \times N_x \times N_y$  is the total lattice sites). For small system sizes with periodic torus geometries, we utilize the ED study with the energy states labeled by the total momentum  $K = (K_x, K_y)$  in units of  $(2\pi/N_x, 2\pi/N_y)$  in the Brillouin zone. For large system

sizes, we exploit finite DMRG on the cylindrical ladder geometry with finite width  $N_y$  and finite length  $N_x$ . We limit the largest width  $N_y = 4$  and length  $N_x = 42$  and keep the maximal bond dimension up to  $M = 4000$ . The boundary condition of cylinder ladder is open in the  $x$  direction and periodic in the  $y$  direction.

## III. THREE-COMPONENT BOSONIC FRACTIONAL QUANTUM HALL EFFECT

In two-dimensional quantum Hall systems, a simple generalization of two-component Halperin's variational wavefunction to higher three-component cases, can be written as (apart from a product factor):

$$\Psi \propto \prod_{i < j, \sigma} (z_i^{\sigma} - z_j^{\sigma})^m \prod_{i, j, \sigma \neq \sigma'} (z_i^{\sigma} - z_j^{\sigma'})^n,$$

whose topological order could be classified by the  $\mathbf{K}$ -matrix

$$\mathbf{K} = \begin{pmatrix} m & n & n \\ n & m & n \\ n & n & m \end{pmatrix}, \quad (4)$$

For simplicity we take complex coordinates  $z_j^{\sigma} = x_j^{\sigma} + iy_j^{\sigma}$  of the  $j$ -th particles with spin- $\sigma$  ( $j = 1, 2, \dots, N_{\sigma}$ ), and suppose the positive values  $m, n > 0$ . From the above equation, we can derive that the first spin- $\sigma$  particle  $z_1^{\sigma}$  hosts the highest orbital angular momentum (also the number of orbital states)  $N_{\phi} = m(N_{\sigma} - 1) + n \sum_{\sigma' \neq \sigma} N_{\sigma'}$  (in units of  $\hbar$ ) in the lowest Landau level under symmetric gauge. Due to cyclic permutation symmetry of the subscript labels,  $N_{\sigma} = N_{\sigma'}$ . For large particle numbers  $N_{\sigma} \gg 1$ , we obtain the spin- $\sigma$  filling  $\nu_{\sigma} = N_{\sigma}/N_{\phi} = 1/(m + 2n)$  and the total particle filling  $\nu = \sum_{\sigma} \nu_{\sigma} = 3/(m + 2n)$ . In connection to our lattice models, we fix the particle fillings of the lowest Chern

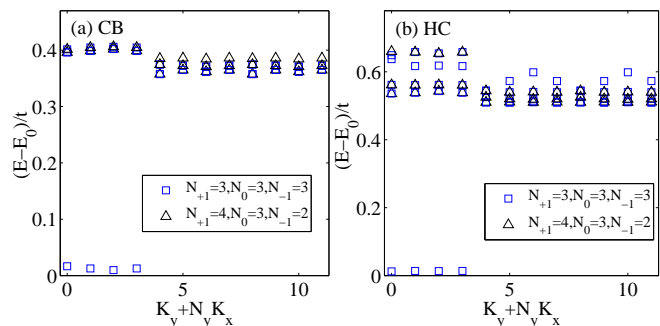


FIG. 1. (Color online) Numerical ED results for the low energy spectrum of three-component hardcore bosons at filling  $\nu = 3/4$  with  $U = \infty$ ,  $V_{\sigma} = 0$ . The system size  $N_s = 2 \times 3 \times 4$  is used for (a) topological checkerboard lattice and (b) topological honeycomb lattice. The lowest four energy levels in each momentum sector are shown.

TABLE I. The total momentum counting in one-dimensional lattice of orbitals of momentum  $k_y + N_y k_x$  for three-component hardcore bosons at filling  $\nu = 3/4$  with  $N_x = 3, N_y = 4$ .

$k_x$	0				1				2				Total Momentum ( $K_x, K_y$ )	
$k_y$	0	1	2	3	0	1	2	3	0	1	2	3	$K_x$	$K_y$
State 1	X	X	X	0	X	X	X	0	X	X	X	0	$9(\text{mod } 3)=0$	$9(\text{mod } 4)=1$
State 2	X	X	0	X	X	X	0	X	X	X	0	X	$9(\text{mod } 3)=0$	$12(\text{mod } 4)=0$
State 3	X	0	X	X	X	0	X	X	X	0	X	X	$9(\text{mod } 3)=0$	$15(\text{mod } 4)=3$
State 4	0	X	X	X	0	X	X	X	0	X	X	X	$9(\text{mod } 3)=0$	$18(\text{mod } 4)=2$

band at  $\nu = \sum_{\sigma} N_{\sigma}/(N_x N_y)$  to simulate the FQH states. Here we consider the FQH states of three-component hardcore bosons at filling  $\nu = 3/4$  under strong onsite repulsions  $U/t \gg 1$  without nearest-neighbor interaction  $V_{\sigma} = 0$ . In the following part we shall characterize the  $\mathbf{K}$  matrix from topological degeneracy, topologically invariant Chern number, and fractional charge pumping.

We take the commensurate finite periodic lattice  $N_s = 2 \times 3 \times 4$  in the ED study with the total particle number  $N = N_{+1} + N_0 + N_{-1} = 9$ . Here we set  $U/t = \infty$  (no more than one particle per site), and the largest reduced Hilbert space is still up to  $1.8 \times 10^8$  in each momentum sector, which would cost the computational memory around 1Tb. As shown in Fig. 1, we plot the low energy spectrum in typical charge sectors  $N_{+1}, N_0, N_{-1}$  for different lattice models, and find that the many-body ground states are four-fold degenerate, with a large robust gap separated from the higher excited levels. Moreover, they fall into the charge sector  $N_{+1} = N_0 = N_{-1}$ , which are of SU(3) spin-singlet nature.

To further unravel the spin-singlet nature, we focus on the charge sectors  $N_{+1} \geq N_0 \geq N_{-1}$ , and define the spin polarization of three-component quantum particles as  $S_z + \delta$  with magnetization  $S_z = \sum_{\sigma} \sigma N_{\sigma}/3$  and relative magnetization  $\delta = (N_{+1} - N_0)/(N_x N_y)$ . As illustrated in Figs. 2(a) and 2(b), we plot the ground state energy of different spin polarizations, and find that the ground state energies satisfy two characteristics: (i)  $E_0(S_z, \delta) < E_0(S'_z, \delta')$  for  $S_z < S'_z$  and (ii)  $E_0(S_z, \delta) <$

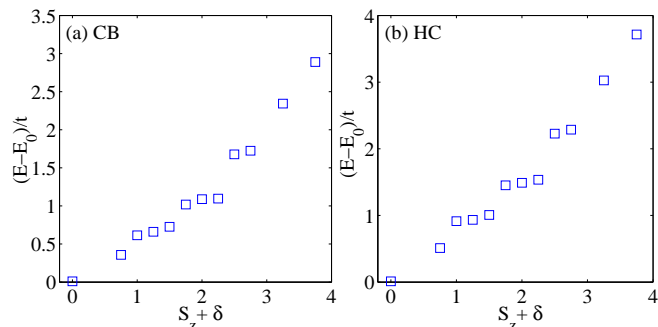


FIG. 2. (Color online) Numerical ED results for the lowest energy level of three-component hardcore bosons at  $\nu = 3/4$  with  $U = \infty, V_{\sigma} = 0$  as a function of spin polarization  $S_z + \delta$  for (a) topological checkerboard lattice and (b) topological honeycomb lattice. The system size  $N_s = 2 \times 3 \times 4$ .

$E_0(S_z, \delta')$  for  $\delta < \delta'$ . Therefore we establish the fact that the lowest energy level always falls into the spin-singlet sector  $S_z = 0, \delta = 0$  (namely  $N_{+1} = N_0 = N_{-1}$ ). Also we note that according to the squeezing rule [58], the four root configurations of SU(3) spin-singlet FQH states at  $\nu = 3/4$  are  $(XXX0)$  and the other translational invariant partners  $(XX0X), (X0XX), (0XXX)$ , where  $XXX$  stands for a superposition of  $|+1\rangle|0\rangle|-1\rangle$  and its five permutation partners  $\sigma \leftrightarrow \sigma'$ . And the total momentum counting by the generalized Pauli principle for the four-fold degenerate ground states for  $N = 9$  particles in a  $N_s = 2 \times 3 \times 4$  lattice is indicated in Table I, and their total momenta are located at  $(K_x, K_y) = (0, i)$  ( $i = 0, 1, 2, 3$ ), consistent with our numerical analysis.

Due to the huge computational memory cost, to overcome the computational difficulty of ED study in calculating topological Chern number, instead we use finite DMRG, and calculate the fractional charge pump to underscore the topological nature, where quantized charge pumping via an adiabatically periodic perturbation is a hallmark of the two-dimensional quantum Hall effect [59], which is connected to the Hall conductance (Chern num-

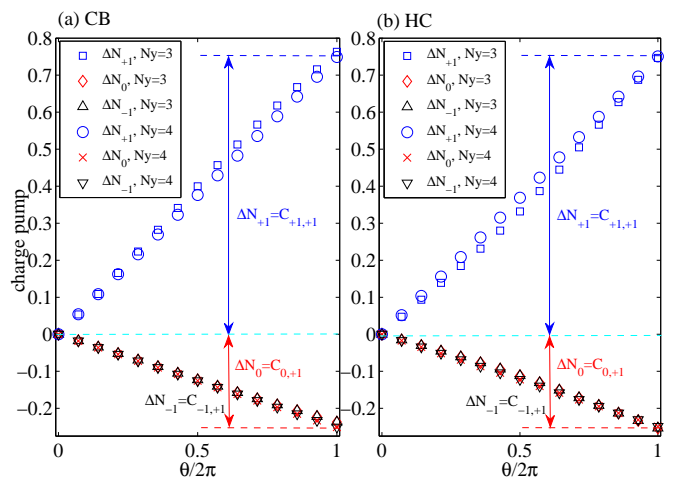


FIG. 3. (Color online) Fractional charge transfers for three-component hardcore bosons at  $\nu = 3/4$  with  $U = \infty, V_{\sigma}/t = 0$ , on the cylinder lattice under the insertion of flux quantum  $\theta_{+1}^y = \theta, \theta_{-1}^y = \theta_{-1}^y = 0$  for two different topological models: (a) checkerboard model and (b) Haldane-honeycomb model. Here finite DMRG is used with different cylinder widths  $N_y = 3, 4$ , keeping the cylinder length up to 40.

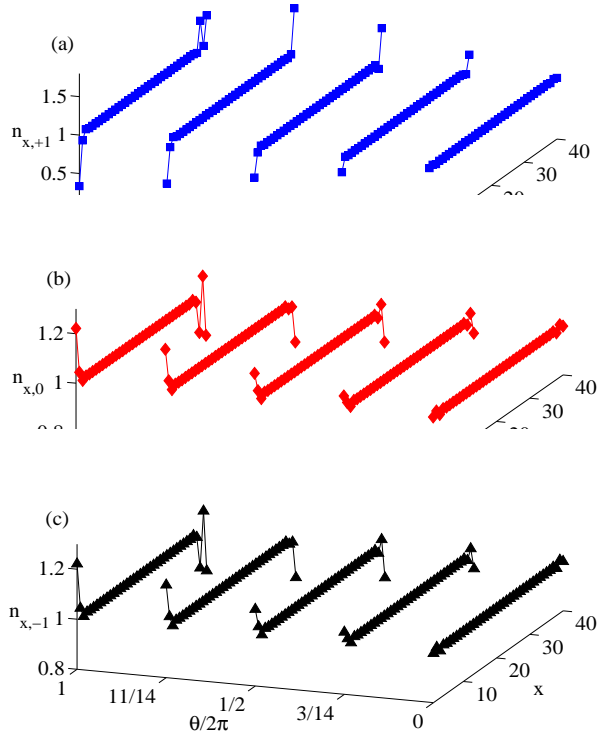


FIG. 4. (Color online) Real-space configurations of particle accumulations  $n_{x,\sigma} = \sum_y n_{\mathbf{r},\sigma}$  in each column for three-component hardcore bosons at  $\nu = 3/4$  with  $U = \infty, V_\sigma/t = 0$ , on the cylinder lattice under the insertion of flux quantum  $\theta_{+1}^y = \theta, \theta_0^y = \theta_{-1}^y = 0$  for topological Haldane-honeycomb model. Here finite DMRG is used with cylinder width  $N_y = 4$  and length  $N_x = 40$ .

ber). Remarkably, for the intercomponent Chern number  $C_{\sigma\sigma'}$ , it is shown that a quantized drag Hall conductance can be obtained by threading one flux quantum (namely, the twisted angle  $\theta_\sigma^y$  changes from zero to  $2\pi$  [60]).

To simulate this physical effect, we utilize finite DMRG to calculate the charge pumping on finite cylinder ladders under the adiabatic insertion of one flux quantum. Numerically we focus on the charge sector  $N_{+1} = N_0 = N_{-1}$ , and cut the finite cylinder into equal left-half and right-half parts along the  $x$  direction. As the twisted angle  $\theta_\sigma^y$  is changed, we define the total particle number of the spin- $\sigma$  component in the right-half part as  $N_\sigma^R(\theta_\sigma^y) = \sum_{\mathbf{r}} n_{\mathbf{r},\sigma}^R$  where  $n_{\mathbf{r},\sigma}^R$  is the occupation number on lattice sites of the right-half part. By tracing the evolution of  $N_\sigma^R(\theta_\sigma^y)$  as a function of  $\theta_\sigma^y$ , we obtain the net charge transfers for the spin- $\sigma$  particle from the left-half side to the right-half side on the cylinder. As illustrated in Figs. 3(a) and 3(b), we plot the evolution of the charge transfer under the insertion of one flux quantum  $\theta_{+1}^y = \theta, \theta_0^y = \theta_{-1}^y = 0$  for two different types of topological lattice models, and find the fractionally quantized

charge pumpings

$$\begin{aligned}\Delta N_{+1} &= N_{+1}^R(2\pi) - N_{+1}^R(0) \simeq C_{+1,+1} = \frac{3}{4}, \\ \Delta N_0 &= N_0^R(2\pi) - N_0^R(0) \simeq C_{0,+1} = -\frac{1}{4}, \\ \Delta N_{-1} &= N_{-1}^R(2\pi) - N_{-1}^R(0) \simeq C_{-1,+1} = -\frac{1}{4}.\end{aligned}$$

We also measure the corresponding real-space configuration of particle accumulation along the cylinder length, defined as  $n_{x,\sigma} = \sum_y n_{\mathbf{r},\sigma}$  (the summation is done over all the  $2N_y$  sites in each column  $x$ ). As shown in Figs. 4(a-c), we find nontrivial edge charge polarization with the increase of  $\theta_\sigma^y$ : the particles of spin- $\sigma$  accumulate at one edge of the cylinder while they diminish at the other edge of the cylinder, which is equivalent to the charge pumping  $C_{\sigma,\sigma'}$  from one edge to the other edge in the above discussion. Because of the permutation symmetry of pseudospin  $c_{\mathbf{r},\sigma} \equiv c_{\mathbf{r},\sigma'}$  in the model Hamiltonian, we obtain the other Chern numbers  $C_{0,0} = C_{-1,-1} = C_{+1,+1}$  and  $C_{\sigma,\sigma'} = C_{\sigma',\sigma}$ . Then the topological  $\mathbf{K}$ -matrix classification is given by the inverse of the Chern number matrix

$$\mathbf{K} = \begin{pmatrix} C_{+1,+1} & C_{+1,0} & C_{+1,-1} \\ C_{0,+1} & C_{0,0} & C_{0,-1} \\ C_{-1,+1} & C_{-1,0} & C_{-1,-1} \end{pmatrix}^{-1} = \begin{pmatrix} 2 & 1 & 1 \\ 1 & 2 & 1 \\ 1 & 1 & 2 \end{pmatrix}. \quad (5)$$

In turn, the determinant of this  $\mathbf{K}$ -matrix  $\det|\mathbf{K}| = 4$  matches with the topological degeneracy of the ground state manifold in our ED study, as required.

#### IV. FRACTIONAL QUANTUM HALL EFFECT OF THREE-COMPONENT BOSE-FERMI MIXTURES

Following the last section, we turn to analyze the emergence of multicomponent FQH effect of three-component Bose-Fermi mixtures, whose topological order could be classified by the symmetric integer-valued  $\mathbf{K}$ -matrix

$$\mathbf{K} = \begin{pmatrix} m_{+1} & n_1 & n_2 \\ n_1 & m_0 & n_3 \\ n_2 & n_3 & m_{-1} \end{pmatrix}, \quad (6)$$

Due to individual quantum statistics of bosons and fermions, the diagonal elements of the  $\mathbf{K}$ -matrix are unequal  $m_\sigma \neq m_{\sigma'}$ . Similar to that in Sec. III, we continue to apply finite DMRG to calculate the charge pumping under the adiabatic insertion of one flux quantum and construct the Chern number matrix.

##### A. Mixture of two-component bosons and one-component fermions

We first investigate a mixture of two-component bosons and one-component fermions in the model Hamiltonian, where the particles of spin- $\sigma = +1, 0$  component

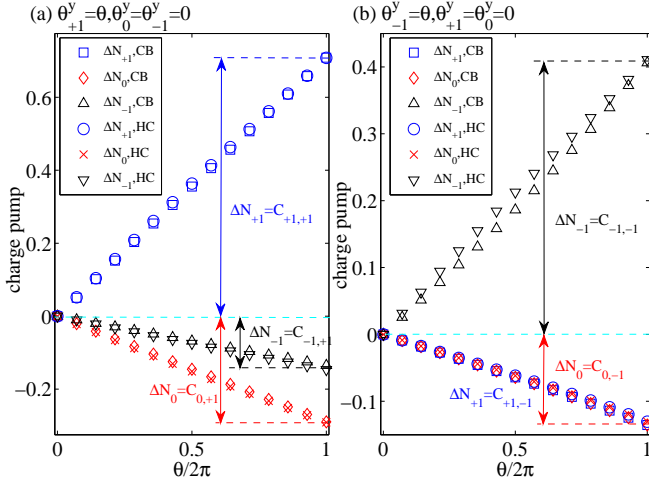


FIG. 5. (Color online) Fractional charge transfers for two-component hardcore bosons at  $\nu_{+1} = \nu_0 = 2/7$  and one-component fermions at  $\nu_{-1} = 1/7$  with  $U = \infty, V_{-1}/t = 100, V_{+1}/t = V_0/t = 0$ , on the cylinder lattice for two different topological models under the insertion of two types of flux quantum: (a)  $\theta_{+1}^y = \theta, \theta_0^y = \theta_{-1}^y = 0$  and (b)  $\theta_{-1}^y = \theta, \theta_{+1}^y = \theta_0^y = 0$ . Here finite DMRG is used with cylinder width  $N_y = 4$  and length  $N_x = 42$ .

are taken as hardcore bosons while the particles of spin- $\sigma = -1$  component are treated as spinless fermions. We consider the FQH states of two-component bosons at fillings  $\nu_{+1} = \nu_0 = 2/7$  and one-component fermions at filling  $\nu_{-1} = 1/7$  with strong onsite repulsions  $U/t \gg 1$  among different components and only intracomponent nearest-neighboring repulsion between fermions (namely  $V_{-1}/t \gg 1$  and  $V_{+1} = V_0 = 0$ ).

As illustrated in Figs. 5(a) and 5(b) for different types of flux insertion in different topological lattice models, we calculate the charge pumpings  $\Delta N_\sigma = N_\sigma^R(\theta_\sigma^y = 2\pi) - N_\sigma^R(\theta_\sigma^y = 0)$  and find that (i) for the flux insertion of spin- $\sigma = +1$  bosons  $\theta_{+1}^y = \theta, \theta_0^y = \theta_{-1}^y = 0, \theta \in [0, 2\pi]$ ,

$$\begin{aligned}\Delta N_{+1} &= N_{+1}^R(2\pi) - N_{+1}^R(0) \simeq C_{+1,+1} = \frac{5}{7}, \\ \Delta N_0 &= N_0^R(2\pi) - N_0^R(0) \simeq C_{0,+1} = -\frac{2}{7}, \\ \Delta N_{-1} &= N_{-1}^R(2\pi) - N_{-1}^R(0) \simeq C_{-1,+1} = -\frac{1}{7}.\end{aligned}$$

and (ii) for the flux insertion of spin- $\sigma = -1$  fermions  $\theta_{+1}^y = \theta_0^y = 0, \theta_{-1}^y = \theta, \theta \in [0, 2\pi]$ ,

$$\begin{aligned}\Delta N_{+1} &= N_{+1}^R(2\pi) - N_{+1}^R(0) \simeq C_{+1,-1} = -\frac{1}{7}, \\ \Delta N_0 &= N_0^R(2\pi) - N_0^R(0) \simeq C_{0,-1} = -\frac{1}{7}, \\ \Delta N_{-1} &= N_{-1}^R(2\pi) - N_{-1}^R(0) \simeq C_{-1,-1} = \frac{3}{7}.\end{aligned}$$

From the permutation symmetry  $c_{\mathbf{r},+1} \leftrightarrow c_{\mathbf{r},0}$ , the diagonal and off-diagonal elements  $C_{0,0} = C_{+1,+1}, C_{0,-1} =$

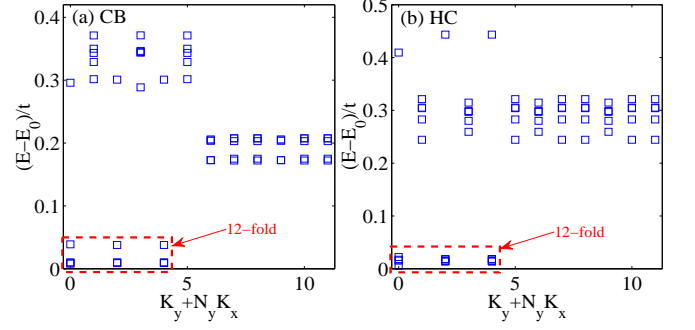


FIG. 6. (Color online) Numerical ED results for the low energy spectrum of one-component hardcore bosons at  $\nu_{+1} = 1/3$  and two-component fermions at  $\nu_{-1} = \nu_0 = 1/6$  with  $U = \infty, V_0/t = V_{-1}/t = 100, V_{+1}/t = 0$ . The system size  $N_s = 2 \times 2 \times 6$  is used for (a) topological checkerboard lattice and (b) topological honeycomb lattice. The lowest five energy levels in each momentum sector are shown. The red dashed box indicates the ground state degeneracy.

$C_{+1,-1}$ . Now we can obtain the  $\mathbf{K}$ -matrix from the inverse of the Chern number matrix, namely

$$\mathbf{K} = \mathbf{C}^{-1} = \begin{pmatrix} 2 & 1 & 1 \\ 1 & 2 & 1 \\ 1 & 1 & 3 \end{pmatrix}. \quad (7)$$

## B. Mixture of one-component bosons and two-component fermions

We further examine a mixture of one-component bosons and two-component fermions in the model Hamiltonian, where the particles of spin- $\sigma = +1$  component are taken as spinless hardcore bosons while the particles of spin- $\sigma = 0, -1$  component are treated as spinful fermions. We would consider the FQH states of one-component bosons at filling  $\nu_{+1} = 1/3$  and two-component fermions at fillings  $\nu_0 = \nu_{-1} = 1/6$  with strong onsite repulsions  $U/t \gg 1$  among different components and only intracomponent nearest-neighboring repulsion between spinful fermions (namely  $V_0/t = V_{-1}/t \gg 1$  and  $V_{+1} = 0$ ). For small system sizes, our ED study of the low energy spectrum indicates a twelve-fold quasi-degenerate ground state manifold, as shown in Figs. 6(a) and 6(b).

For larger system sizes, as shown in Figs. 7(a) and 7(b), we plot the evolution of charge transfers for different types of flux insertion in different topological lattice models, and find that (i) for the flux insertion of spin- $\sigma = +1$  bosons  $\theta_{+1}^y = \theta, \theta_0^y = \theta_{-1}^y = 0, \theta \in [0, 2\pi]$ , the charge



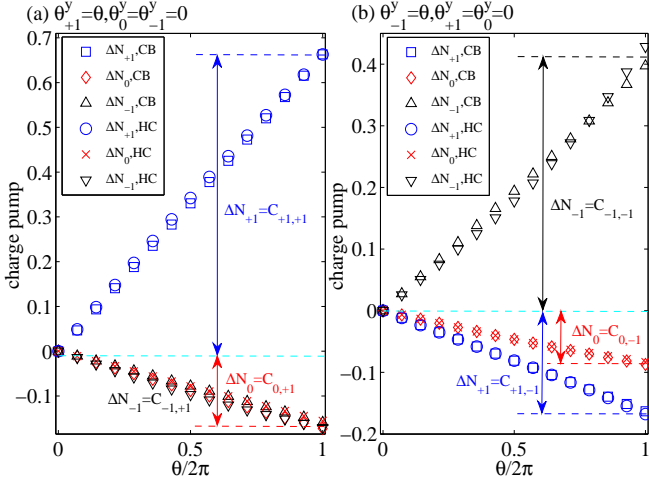


FIG. 7. (Color online) Fractional charge transfers for one-component hardcore bosons at  $\nu_{+1} = 1/3$  and two-component fermions at  $\nu_{-1} = \nu_0 = 1/6$  with  $U = \infty, V_0/t = V_{-1}/t = 100, V_{+1}/t = 0$ , on the cylinder lattice for two different topological models under the insertion of two types of flux quantum: (a)  $\theta_{+1}^y = \theta, \theta_0^y = \theta_{-1}^y = 0$  and (b)  $\theta_{-1}^y = \theta, \theta_{+1}^y = \theta_0^y = 0$ . Here finite DMRG is used with cylinder width  $N_y = 4$  and length  $N_x = 42$ .

pumpings

$$\begin{aligned}\Delta N_{+1} &= N_{+1}^R(2\pi) - N_{+1}^R(0) \simeq C_{+1,+1} = \frac{2}{3}, \\ \Delta N_0 &= N_0^R(2\pi) - N_0^R(0) \simeq C_{0,+1} = -\frac{1}{6}, \\ \Delta N_{-1} &= N_{-1}^R(2\pi) - N_{-1}^R(0) \simeq C_{-1,+1} = -\frac{1}{6}.\end{aligned}$$

and (ii) for the flux insertion of spin- $\sigma = -1$  fermions, the charge pumpings  $\theta_{+1}^y = \theta_0^y = 0, \theta_{-1}^y = \theta, \theta \subseteq [0, 2\pi]$ ,

$$\begin{aligned}\Delta N_{+1} &= N_{+1}^R(2\pi) - N_{+1}^R(0) \simeq C_{+1,-1} = -\frac{1}{6}, \\ \Delta N_0 &= N_0^R(2\pi) - N_0^R(0) \simeq C_{0,-1} = -\frac{1}{12}, \\ \Delta N_{-1} &= N_{-1}^R(2\pi) - N_{-1}^R(0) \simeq C_{-1,-1} = \frac{5}{12}.\end{aligned}$$

As above we can obtain the  $\mathbf{K}$ -matrix from the inverse of the Chern number matrix, namely

$$\mathbf{K} = \mathbf{C}^{-1} = \begin{pmatrix} 2 & 1 & 1 \\ 1 & 3 & 1 \\ 1 & 1 & 3 \end{pmatrix}. \quad (8)$$

The determinant of this  $\mathbf{K}$ -matrix also matches with the topological degeneracy of the ground state manifold in our ED study correspondingly.

## V. NON-ABELIAN SPIN-SINGLET FRACTIONAL QUANTUM HALL EFFECT

In this section, we extend our technique to identify non-Abelian  $SU(3)$  spin-singlet FQH states for three-

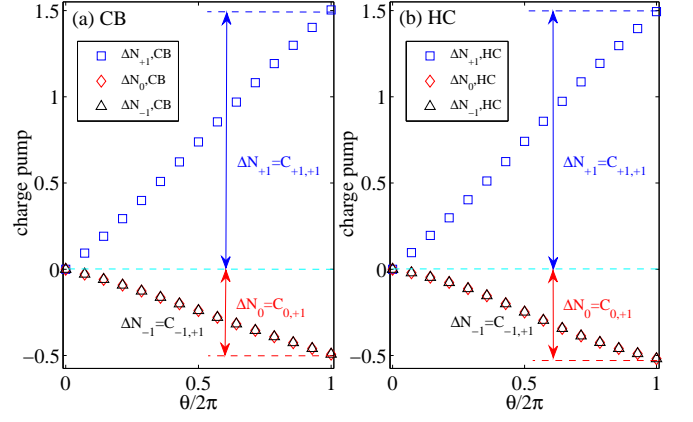


FIG. 8. (Color online) Fractional charge transfers for three-component softcore bosons at  $\nu = 3/2$  with infinite three-body repulsion  $U_{3b} = \infty$  on the cylinder lattice under the insertion of flux quantum  $\theta_{+1}^y = \theta, \theta_0^y = \theta_{-1}^y = 0$  for two different topological models: (a) checkerboard model and (b) Haldane-honeycomb model. Here finite DMRG is used with different cylinder widths  $N_y = 3$ , keeping the cylinder length up to 36.

component softcore bosons at filling  $\nu = 3k/4$  in the presence of  $(k+1)$ -body interactions as a primary example [61]. Following Ref. [24], we can construct the trial wavefunction (apart from a constant conformal product factor) from that of Abelian  $SU(3)$  FQH state at  $\nu = 3/4$  as

$$\begin{aligned}\Psi_{\nu=3k/4} &\propto [\Psi_{\nu=3/4}]^{1/k} \\ &\propto \prod_{i<j,\sigma} (z_i^\sigma - z_j^\sigma)^{2/k} \prod_{i,j,\sigma \neq \sigma'} (z_i^\sigma - z_j^{\sigma'})^{1/k}.\end{aligned} \quad (9)$$

Akin to two-component non-Abelian spin-singlet states as discussed in Ref. [62], we claim a peculiar  $3 \times 3$  Chern-number matrix, in connection with the power-law exponents of mutual particle correlations in Eq. 9,

$$\mathbf{C} = \frac{k}{4} \begin{pmatrix} 3 & -1 & -1 \\ -1 & 3 & -1 \\ -1 & -1 & 3 \end{pmatrix} = \begin{pmatrix} 2/k & 1/k & 1/k \\ 1/k & 2/k & 1/k \\ 1/k & 1/k & 2/k \end{pmatrix}^{-1} \quad (10)$$

Numerically, we here mainly discuss the simplest case of  $k = 2$  with  $SU(3)$  symmetric three-body repulsion in Eqs. 1 and 2,

$$V_{int} = U_{3b} \sum_{\mathbf{r}} \prod_{i=0}^{k=2} (n_{\mathbf{r},+1} + n_{\mathbf{r},0} + n_{\mathbf{r},-1} - i) \quad (11)$$

In the strongly interacting regime  $U_{3b} = \infty$  (namely no more than  $k = 2$  particles are allowed per lattice site), our DMRG simulation of the charge pumping on finite cylinder ladders by inserting one flux quantum  $\theta_{+1}^y = \theta, \theta_0^y = \theta_{-1}^y = 0, \theta \subseteq [0, 2\pi]$ , as shown in Figs. 8(a)

and 8(b), gives

$$\begin{aligned}\Delta N_{+1} &= N_{+1}^R(2\pi) - N_{+1}^R(0) \simeq C_{+1,+1} = \frac{3}{2}, \\ \Delta N_0 &= N_0^R(2\pi) - N_0^R(0) \simeq C_{0,+1} = -\frac{1}{2}, \\ \Delta N_{-1} &= N_{-1}^R(2\pi) - N_{-1}^R(0) \simeq C_{-1,+1} = -\frac{1}{2},\end{aligned}$$

which coincide with the prediction of Eq. 10. Thus, our formulation of the Chern number matrix faithfully manifests the internal structure of non-Abelian multicomponent FQH state here.

## VI. CONCLUSION

To summarize our findings, we have developed a controllable scheme for studying three-component FQH effects emerging in paradigmatic topological lattice models under the interplay of band topology, intercomponent and intracomponent correlations. We numerically uncover the  $\mathbf{K}$ -matrix classifications at filling  $\nu = 3/4$  for three-component hardcore bosons and at various fillings for three-component Bose-Fermi mixtures. We implement this by providing two pieces of major ingredients: (i)  $\det|\mathbf{K}|$ -fold ground state manifold equivalent to the determinant of the  $\mathbf{K}$  matrix from ED calculation, (ii) topological Chern number matrix equivalent to the inverse of the  $\mathbf{K}$  matrix from DMRG calculation. We also propose a Chern number matrix to characterize non-Abelian three-component spin-singlet FQH effect. It is noteworthy that our comprehensive DMRG simulation of fractional charge pumping of multicomponent systems reveals a wealth of crucial information about the topological order, ultimately serving as a practical tool for

probing exotic quantum Hall physics.

## ACKNOWLEDGMENTS

T.S.Z thanks D. N. Sheng and W. Zhu for inspiring discussions and prior collaborations on multicomponent fractional quantum Hall physics in topological flat band models. This work is supported by the National Natural Science Foundation of China (NSFC) under Grant No. 12074320.

## Appendix A: Chern number matrix

In interacting systems, topological Chern number of the many-body ground state can be obtained using twisted boundary conditions  $c_{\mathbf{r}+N_{\alpha},\sigma} = c_{\mathbf{r},\sigma} \exp(i\theta_{\sigma}^{\alpha})$  in the  $\alpha = x, y$  direction where  $\theta_{\sigma}^{\alpha}$  is the twisted angle which leads to a shift of lattice momentum  $k_{\alpha} \rightarrow k_{\alpha} + \theta_{\sigma}^{\alpha}/N_{\alpha}$  in the spin- $\sigma$  component [63]. In the parameter plane of two independent twisted angles  $\theta_{\sigma}^x \subseteq [0, 2\pi]$ ,  $\theta_{\sigma'}^y \subseteq [0, 2\pi]$ , the Chern number of the many-body ground state wavefunction  $\psi(\theta_{\sigma}^x, \theta_{\sigma'}^y)$  is defined by the integral formula  $C_{\sigma\sigma'} = \int \int d\theta_{\sigma}^x d\theta_{\sigma'}^y F_{\sigma\sigma'}(\theta_{\sigma}^x, \theta_{\sigma'}^y)/2\pi$ , where the Berry curvature  $F_{\sigma\sigma'}(\theta_{\sigma}^x, \theta_{\sigma'}^y) = \mathbf{Im} \left( \langle \frac{\partial \psi}{\partial \theta_{\sigma}^x} | \frac{\partial \psi}{\partial \theta_{\sigma'}^y} \rangle - \langle \frac{\partial \psi}{\partial \theta_{\sigma'}^y} | \frac{\partial \psi}{\partial \theta_{\sigma}^x} \rangle \right)$ . For three-component systems, we can write down nine elementary Chern numbers  $C_{\sigma\sigma'}$  for  $\sigma, \sigma' = 0, \pm 1$ , which constitute a Chern number matrix spanned in spin space [64, 65]

$$\mathbf{C} = \begin{pmatrix} C_{+1,+1} & C_{+1,0} & C_{+1,-1} \\ C_{0,+1} & C_{0,0} & C_{0,-1} \\ C_{-1,+1} & C_{-1,0} & C_{-1,-1} \end{pmatrix}. \quad (\text{A1})$$

- 
- [1] B. I. Halperin, *Theory of the quantized Hall conductance*, Helv. Phys. Acta, **56**, 75 (1983).
- [2] X.-G. Wen and A. Zee, *Neutral superfluid modes and "magnetic" monopoles in multilayered quantum Hall systems*, Phys. Rev. Lett. **69**, 1811 (1992).
- [3] T. Chakraborty and P. Pietiläinen, *Fractional Quantum Hall Effect at Half-Filled Landau Level in a Multiple-Layer Electron System*, Phys. Rev. Lett. **59**, 2784 (1987).
- [4] D. Yoshioka, A. H. MacDonald, and S. M. Girvin, *Connection between spin-singlet and hierarchical wave functions in the fractional quantum Hall effect*, Phys. Rev. B **38**, 3636(R) (1988).
- [5] D. Yoshioka, A. H. MacDonald, and S. M. Girvin, *Fractional quantum Hall effect in two-layered systems*, Phys. Rev. B **39**, 1932 (1989).
- [6] S. He, X. C. Xie, S. Das Sarma, and F. C. Zhang, *Quantum Hall effect in double-quantum-well systems*, Phys. Rev. B **43**, 9339(R) (1991).
- [7] S. He, S. Das Sarma, and X. C. Xie, *Quantized Hall effect and quantum phase transitions in coupled two-layer electron systems*, Phys. Rev. B **47**, 4394 (1993).
- [8] A. Seidel and K. Yang, *Halperin ( $m, m', n$ ) Bilayer Quantum Hall States on Thin Cylinders*, Phys. Rev. Lett. **101**, 036804 (2008).
- [9] K. I. Bolotin, F. Ghahari, M. D. Shulman, H. L. Stormer, and P. Kim, *Observation of the fractional quantum Hall effect in graphene*, Nature (London) **462**, 196 (2009).
- [10] C. Dean, A. Young, P. Cadden-Zimansky, L. Wang, H. Ren, K. Watanabe, T. Taniguchi, P. Kim, J. Hone, and K. Shepard, *Multicomponent fractional quantum Hall effect in graphene*, Nat. Phys. **7**, 693 (2011).
- [11] C. Töke and J. K. Jain, *SU(4) composite fermions in graphene: Fractional quantum Hall states without analog in GaAs*, Phys. Rev. B **75**, 245440 (2007).
- [12] M. O. Goerbig and N. Regnault, *Analysis of a SU(4) generalization of Halperin's wave function as an approach towards a SU(4) fractional quantum Hall effect in graphene sheets*, Phys. Rev. B **75**, 241405(R) (2007).
- [13] R. de Gail, N. Regnault, and M. O. Goerbig, *Plasma picture of the fractional quantum Hall effect with internal SU(K) symmetries*, Phys. Rev. B **77**, 165310 (2008).

- [14] X.-G. Wen, *Zoo of quantum-topological phases of matter*, Rev. Mod. Phys. **89**, 041004 (2017).
- [15] X. Liu, Z. Hao, K. Watanabe, T. Taniguchi, B. I. Halperin, and P. Kim, *Interlayer fractional quantum Hall effect in a coupled graphene double layer*, Nature Phys. **15**, 893 (2019).
- [16] J. I. A. Li, Q. Shi, Y. Zeng, K. Watanabe, T. Taniguchi, J. Hone, and C. R. Dean, *Pairing states of composite fermions in double-layer graphene*, Nature Phys. **15**, 898 (2019).
- [17] T. Graß, B. Juliá-Díaz, N. Barberán, and M. Lewenstein, *Non-Abelian spin-singlet states of two-component Bose gases in artificial gauge fields*, Phys. Rev. A **86**, 021603(R) (2012).
- [18] S. Furukawa and M. Ueda, *Quantum Hall states in rapidly rotating two-component Bose gases*, Phys. Rev. A **86**, 031604(R) (2012).
- [19] Y.-H. Wu and J. K. Jain, *Quantum Hall effect of two-component bosons at fractional and integral fillings*, Phys. Rev. B **87**, 245123 (2013).
- [20] T. Graß, D. Raventós, M. Lewenstein, and B. Juliá-Díaz, *Quantum Hall phases of two-component bosons*, Phys. Rev. B **89**, 045114 (2014).
- [21] T. Senthil and M. Levin, *Integer Quantum Hall Effect for Bosons*, Phys. Rev. Lett. **110**, 046801 (2013).
- [22] S. Furukawa and M. Ueda, *Integer Quantum Hall State in Two-Component Bose Gases in a Synthetic Magnetic Field*, Phys. Rev. Lett. **111**, 090401 (2013).
- [23] N. Regnault and T. Senthil, *Microscopic model for the boson integer quantum Hall effect*, Phys. Rev. B **88**, 161106(R) (2013).
- [24] E. Ardonne and K. Schoutens, *New Class of Non-Abelian Spin-Singlet Quantum Hall States*, Phys. Rev. Lett. **82**, 5096 (1999).
- [25] J. W. Reijnders, F. J. M. van Lankvelt, K. Schoutens, and N. Read, *Quantum Hall States and Boson Triplet Condensate for Rotating Spin-1 Bosons*, Phys. Rev. Lett. **89**, 120401 (2002).
- [26] M. Barkeshli and X.-G. Wen, *Classification of Abelian and non-Abelian multilayer fractional quantum Hall states through the pattern of zeros*, Phys. Rev. B **82**, 245301 (2010).
- [27] F. Wu, I. Sodemann, A. H. MacDonald, and T. Jolicœur, *SU(3) and SU(4) Singlet Quantum Hall States at  $\nu = 2/3$* , Phys. Rev. Lett. **115**, 166805 (2015).
- [28] W. Zhao, K. Kang, Y. Zhang, P. Knüppel, Z. Tao, L. Li, C. L. Tschirhart, E. Redekop, K. Watanabe, T. Taniguchi, A. F. Young, J. Shan and K. F. Mak, *Realization of the Haldane Chern insulator in a moiré lattice*, Nature Phys. **20**, 275 (2024).
- [29] H. Park, J. Cai, E. Anderson, Y. Zhang, J. Zhu, X. Liu, C. Wang, W. Holtzmann, C. Hu, Z. Liu, T. Taniguchi, K. Watanabe, J.-H. Chu, T. Cao, L. Fu, W. Yao, C.-Z. Chang, D. Cobden, D. Xiao and X. Xu, *Observation of fractionally quantized anomalous Hall effect*, Nature **622**, 74 (2023).
- [30] K. Kang, B. Shen, Y. Qiu, Y. Zeng, Z. Xia, K. Watanabe, T. Taniguchi, J. Shan and K. F. Mak, *Evidence of the fractional quantum spin Hall effect in moiré MoTe<sub>2</sub>*, Nature **628**, 526 (2024).
- [31] Z. Liu, E. J. Bergholtz, H. Fan, A. M. Läuchli, *Fractional Chern Insulators in Topological Flat Bands with Higher Chern Number*, Phys. Rev. Lett. **109**, 186805 (2012).
- [32] Y.-F. Wang, H. Yao, C.-D. Gong, and D. N. Sheng, *Fractional quantum Hall effect in topological flat bands with Chern number two*, Phys. Rev. B **86**, 201101(R) (2012).
- [33] S. Yang, Z.-C. Gu, K. Sun, and S. Das Sarma, *Topological flat band models with arbitrary Chern numbers*, Phys. Rev. B **86**, 241112(R) (2012).
- [34] A. Sterdyniak, C. Repellin, B. A. Bernevig, and N. Regnault, *Series of Abelian and non-Abelian states in  $C > 1$  fractional Chern insulators*, Phys. Rev. B **87**, 205137 (2013).
- [35] Y.-L. Wu, N. Regnault, and B. A. Bernevig, *Bloch Model Wave Functions and Pseudopotentials for All Fractional Chern Insulators*, Phys. Rev. Lett. **110**, 106802 (2013).
- [36] Y.-L. Wu, N. Regnault, and B. A. Bernevig, *Haldane statistics for fractional Chern insulators with an arbitrary Chern number*, Phys. Rev. B **89**, 155113 (2014).
- [37] Y.-H. Wu, J. K. Jain, and K. Sun, *Fractional topological phases in generalized Hofstadter bands with arbitrary Chern numbers*, Phys. Rev. B **91**, 041119(R) (2015).
- [38] B. Andrews and G. Möller, *Stability of fractional Chern insulators in the effective continuum limit of Harper-Hofstadter bands with Chern number  $|C| > 1$* , Phys. Rev. B **97**, 035159 (2018).
- [39] T.-S. Zeng, W. Zhu, and D. N. Sheng, *Two-component quantum Hall effects in topological flat bands*, Phys. Rev. B **95**, 125134 (2017).
- [40] T.-S. Zeng and D. N. Sheng, *SU(N) fractional quantum Hall effect in topological flat bands*, Phys. Rev. B **97**, 035151 (2018).
- [41] T.-S. Zeng, D. N. Sheng, and W. Zhu, *Topological characterization of hierarchical fractional quantum Hall effects in topological flat bands with SU(N) symmetry*, Phys. Rev. B **100**, 075106 (2019).
- [42] T.-S. Zeng, D. N. Sheng, and W. Zhu, *Quantum Hall effects of exciton condensate in topological flat bands*, Phys. Rev. B **101**, 195310 (2020).
- [43] T.-S. Zeng, L. Hu, and W. Zhu, *Bosonic Halperin (441) fractional quantum Hall effect at filling factor  $\nu = 2/5$* , Chin. Phys. Lett. **39**, 017301 (2022).
- [44] T.-S. Zeng, *Integer quantum Hall effect of two-component hard-core bosons in a topological triangular lattice*, Phys. Rev. B **105**, 235140 (2022).
- [45] X. G. Wen and A. Zee, *Classification of Abelian quantum Hall states and matrix formulation of topological fluids*, Phys. Rev. B **46**, 2290 (1992).
- [46] X. G. Wen and A. Zee, *Shift and spin vector: New topological quantum numbers for the Hall fluids*, Phys. Rev. Lett. **69**, 953 (1992).
- [47] B. Blok and X. G. Wen, *Effective theories of the fractional quantum Hall effect at generic filling fractions*, Phys. Rev. B **42**, 8133 (1990).
- [48] B. Blok and X. G. Wen, *Effective theories of the fractional quantum Hall effect: Hierarchy construction*, Phys. Rev. B **42**, 8145 (1990).
- [49] B. Blok and X. G. Wen, *Structure of the microscopic theory of the hierarchical fractional quantum Hall effect*, Phys. Rev. B **43**, 8337 (1991).
- [50] L. Hu, Z. Liu, and W. Zhu, *Modular transformation and anyonic statistics of multicomponent fractional quantum Hall states*, Phys. Rev. B **108**, 235121 (2023).
- [51] Y.-H. Wu, *Chiral topological states in Bose-Fermi mixtures*, Phys. Rev. B **99**, 125108 (2019).
- [52] T.-S. Zeng, *Fractional quantum Hall effect of Bose-Fermi mixtures*, Phys. Rev. B **103**, L201118 (2021).



- [53] K. Sun, Z. Gu, H. Katsura, and S. Das Sarma, *Nearly Flatbands with Nontrivial Topology*, Phys. Rev. Lett. **106**, 236803 (2011).
- [54] Y.-F. Wang, Z.-C. Gu, C.-D. Gong, and D. N. Sheng, *Fractional Quantum Hall Effect of Hard-Core Bosons in Topological Flat Bands*, Phys. Rev. Lett. **107**, 146803 (2011).
- [55] Q. Niu, D. J. Thouless, and Y.-S. Wu, *Quantized Hall conductance as a topological invariant*, Phys. Rev. B **31**, 3372 (1985).
- [56] D. N. Sheng, L. Balents, and Z. Wang, *Phase Diagram for Quantum Hall Bilayers at  $\nu = 1$* , Phys. Rev. Lett. **91**, 116802 (2003).
- [57] D. N. Sheng, Z.-Y. Weng, L. Sheng, and F. D. M. Haldane, *Quantum Spin-Hall Effect and Topologically Invariant Chern Numbers*, Phys. Rev. Lett. **97**, 036808 (2006).
- [58] E. Ardonne and N. Regnault, *Structure of spinful quantum Hall states: A squeezing perspective*, Phys. Rev. B **84**, 205134 (2011).
- [59] R. B. Laughlin, *Quantized Hall conductivity in two dimensions*, Phys. Rev. B **23**, 5632(R) (1981).
- [60] S. S. Gong, W. Zhu, and D. N. Sheng, *Emergent Chiral Spin Liquid: Fractional Quantum Hall Effect in a Kagome Heisenberg Model*, Sci. Rep. **4**, 6317 (2014).
- [61] Y. Fuji and P. Lecheminant, *Non-Abelian  $SU(N - 1)$ -singlet fractional quantum Hall states from coupled wires*, Phys. Rev. B **95**, 125130 (2017).
- [62] T.-S. Zeng and W. Zhu, *Chern-number matrix of the non-Abelian spin-singlet fractional quantum Hall effect*, Phys. Rev. B **105**, 125128 (2022).
- [63] Q. Niu, D. J. Thouless, and Y.-S. Wu, *Quantized Hall conductance as a topological invariant*, Phys. Rev. B **31**, 3372 (1985).
- [64] D. N. Sheng, L. Balents, and Z. Wang, *Phase Diagram for Quantum Hall Bilayers at  $\nu = 1$* , Phys. Rev. Lett. **91**, 116802 (2003).
- [65] D. N. Sheng, Z.-Y. Weng, L. Sheng, and F. D. M. Haldane, *Quantum Spin-Hall Effect and Topologically Invariant Chern Numbers*, Phys. Rev. Lett. **97**, 036808 (2006).